SUPPLEMENTARY INFORMATION

Nanocellulose with Dual Carboxy and Aldehyde Functionality: a Modular Platform for Hydrogel Formation and Sustained Drug Release

Emanuela Bua,[†a] Chiara Spanu,[†a] Giovanni Inzalaco,[b] Martina Zangari,[a] Luca Sartorelli,[a] Letizia Sambri,[a] Elisabetta Venuti,[a] Tommaso Salzillo,[a] Mauro Comes Franchini,[a] Mario Chiariello[c,d] and Erica Locatelli*[a].

a) Department of Industrial Chemistry "Toso Montanari", Via Gobetti 85, 40129, Bologna, Italy.
b) Institute of Endotypes in Oncology, Metabolism and Immunology "Gaetano Salvatore", National Research Council, Via Pansini 5, 80131, Napoli, Italy.
c) Institute of Clinical Physiology, National Research Council, Via Fiorentina 1, 53100, Siena, Italy.
d) Core Research Laboratory (CRL), Istituto per lo Studio la Prevenzione e la Rete Oncologica (ISPRO), Via Fiorentina 1, 53100, Siena, Italy.

[†] These authors contributed equally to the work

* Corresponding author email: erica.locatelli2@unibo.it

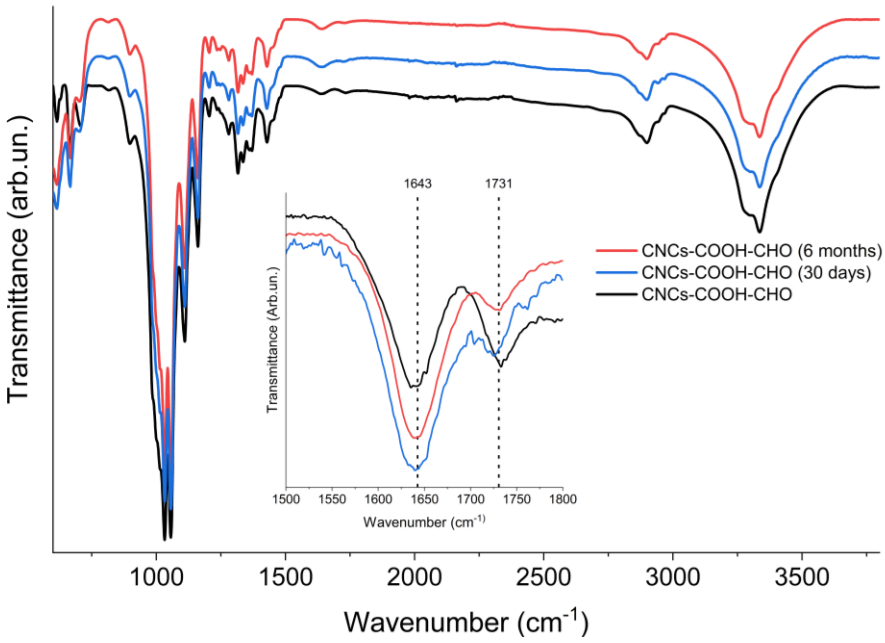

Fig. S1 *ATR-FTIR spectra of CNCs-COOH-CHO analysed after synthesis (black line), after 30 days at 4°C (blue line) and after 6 months stored at rt in freeze-dried form (red line).*

ATR-FTIR band assignments for pristine CNCs. To support the interpretation of the oxidation-induced spectral changes reported in the main text, the principal ATR-FTIR bands of pristine CNCs were assigned based on literature data.[1–3] The characteristic cellulose bands are observed in the fingerprint region and in the O–H stretching region, and their positions remain substantially unchanged after oxidation, indicating that the cellulose backbone is preserved. The main diagnostic bands used to discuss CNC oxidation (carboxyl C=O at 1721 cm-1 for CNCs-COOH and aldehyde C=O at 1733 cm-1 for CNCs-COOH-CHO) are discussed in the main text; additional assignments for the typical CNC vibrational features are reported in Table S1.

Table S1 *Main ATR-FTIR bands of pristine CNCs and literature-based assignments.*[1–3]

Wavenumber (cm^{-1})	**Assignment**	**Notes**
666	C–OH out-of-plane bending	Typical CNC band
710	CH_2 rocking	Typical CNC band
998	C–H ring vibrations	Fingerprint region
1021	C–O–C stretching	Fingerprint region
1031	C–OH stretching	Fingerprint region
1060	C–C vibrations	Fingerprint region
1376	CH_2 bending	Typical CNC band
1644	CH_2–O–H bending or H–O–H bending of adsorbed water	Band commonly observed in CNCs
3292	O–H stretching (intermolecular H-bonding)	Broad band
3335	O–H stretching (intramolecular H-bonding)	Broad band

Table S2 *Zeta potential measurements and average zeta potential of different batches.*

	Zeta potential batch 1	Zeta potential batch 2	Zeta potential batch 3	Average zeta potential
CNCs	(-27.9 ± 8.78) mV	(-30.3 ± 7.04) mV	(-23.9 ± 9.18) mV	(-27.9 ± 4.71) mV
CNCs-COOH	(-45.0 ± 5.66) mV	(-37.9 ± 6.09) mV	(-45.6 ± 8.28) mV	(-42.5 ± 3.71) mV
CNCs-COOH-CHO	(- 37.7 ± 6.56) mV	(-33.6 ± 7.94) mV	(-32.0 ± 6.84) mV	(-34.6 ± 4.07) mV

Table S3 *Different reaction conditions tested in TEMPO-oxidation of CNCs to obtain CNCs-COOH and carboxylate content determined through conductometric titrations.*

	mmol NaClO/g CNCs	Reaction time (min)	Carboxylate content (mmol/g) - sample 1	Carboxylate content (mmol/g) - sample 2	Carboxylate content (mmol/g) - sample 3
CNCs-OX 1	6	50	0.045	0.042	0.041
CNCs-OX 2	10	50	0.101	0.09958	0.071
CNCs-OX 3	10	90	0.381	0.31	0.389

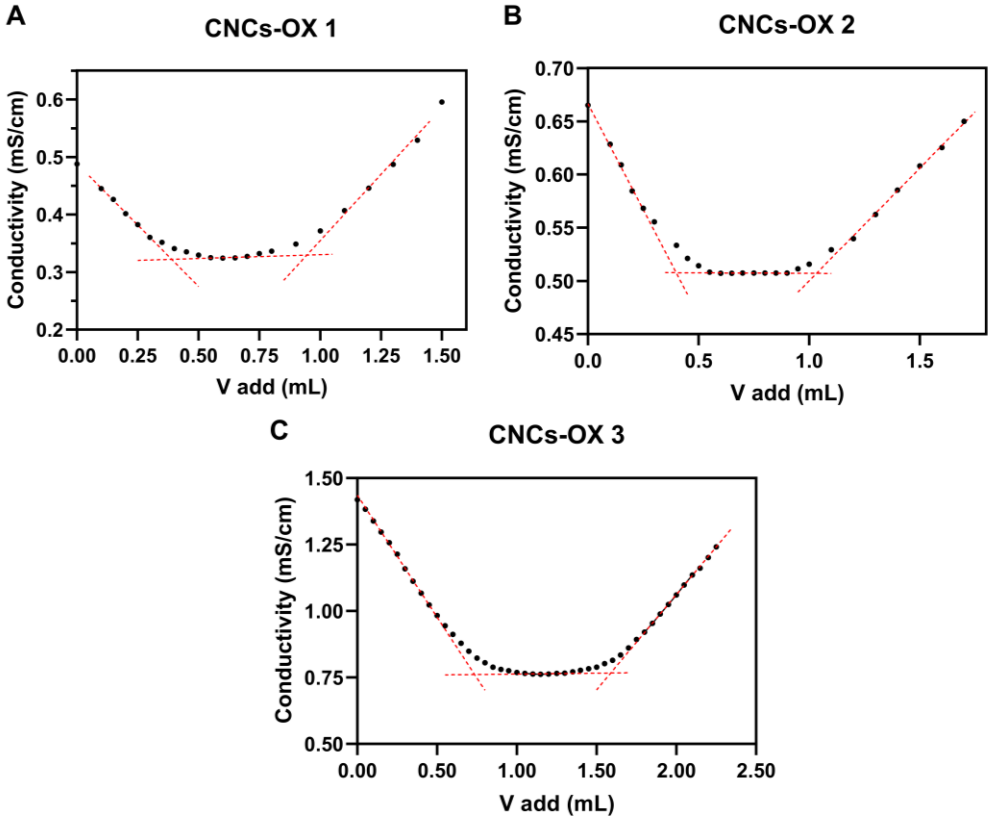

Fig. S2 *Conductometric titration to quantify carboxylated groups on CNCs-COOH related to reactions CNCs-OX1* ***(A)****, CNCs-OX2* ***(B)*** *and CNCs-OX3* ***(C)****.*

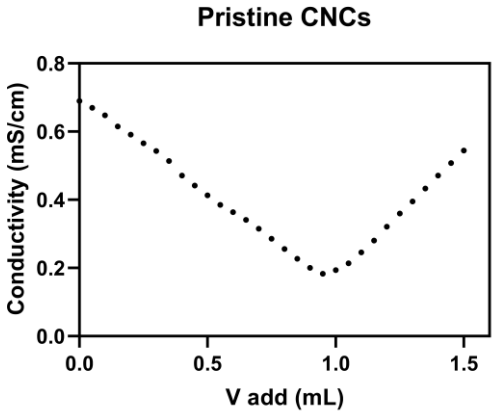

Fig. S3 *Conductometric titration carried out on pristine CNCs.*

Aldehydes Quantification Test. The amount of aldehyde content in CNCs-COOH-CHO was determined by a fluorometric method after performing Hantzsch reaction (Fig. S4). Five-standard solution for the calibration curve and a series of oxidised CNCs samples in a 10 mL volumetric flask were prepared as follows: 5 mL of 4M Ammonium Acetate (AA), 2 mL of 0.2M Acetoacetanilide (AAA) in EtOH, 2 mL of ethanol and a series of *4-chlorobenzaldehyde* 5mM in EtOH or oxidised CNCs samples (A). To reach 10 mL of final volume, the required quantities of H_2O were added and the mixture left under stirring overnight at room temperature. Fluorescence intensities of the reagent blank, *4-chlorobenzaldehyde* standards, and sample solutions were recorded at 470 nm with excitation at 370 nm. Aldehyde concentrations were then calculated using the corresponding calibration curve. (**λ_{exc} = 370 nm; λ_{em} = 452 nm;** filter of 420 nm; Δλ = 2).

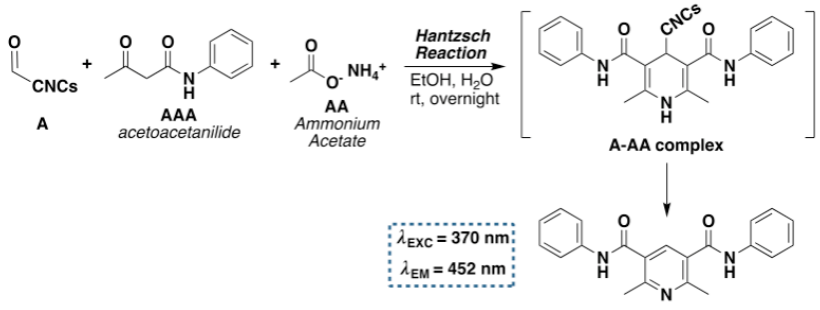

Fig. S4 *Hantzsch reaction for aldehyde quantification.*

Table S4. Left: *Concentrations of 4-chlorobenzaldehyde standards prepared to build the calibration curve for the aldehydes' quantification.* ***Right:*** *Information of the calibration line used to determine the concentration of aldehydes in unknown samples of oxidised nanocellulose (CNCs-CHO).*

Standard	[A] µM
Std 1	5
Std 2	10
Std 3	20
Std 4	50

Calibration Line	
Slope	1.139E+02
Intercept	1.779E+03
R^2	0.989
Sample	**mmolCHO/gCNCs**
CNCs - CHO	**0.277996**

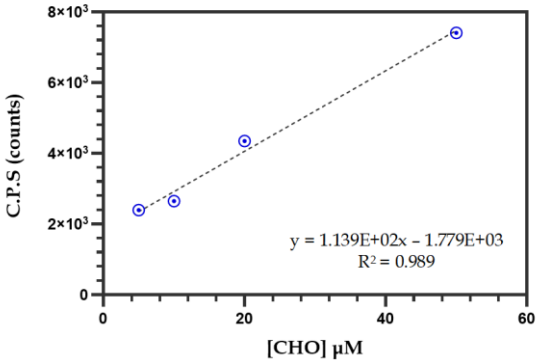

CHO content = 0.278 $\frac{mmol_{CHO}}{g_{CNCs}}$

Fig. S5 *Calibration curve obtained by standard solutions presented in Table S4.*

Table S5. *Hydrogels' composition. Amount of reagents used for hydrogels' formulation.*

	P1	P2	P3	P4	C1	C2	C3	C4
Spermine (mg/mL)	25	25	–	–	2	2	–	–
ε-Poly-L-lysine (mg/mL)	–	–	1.3	1.3	–	–	1.7	1.7
EDC/NHS (mg)	–	–	–	–	39/23	39/23	39/23	39/23
$CaCl_2$ (mg/mL)	0.3	0.3	–	–	0.09	0.09	–	–

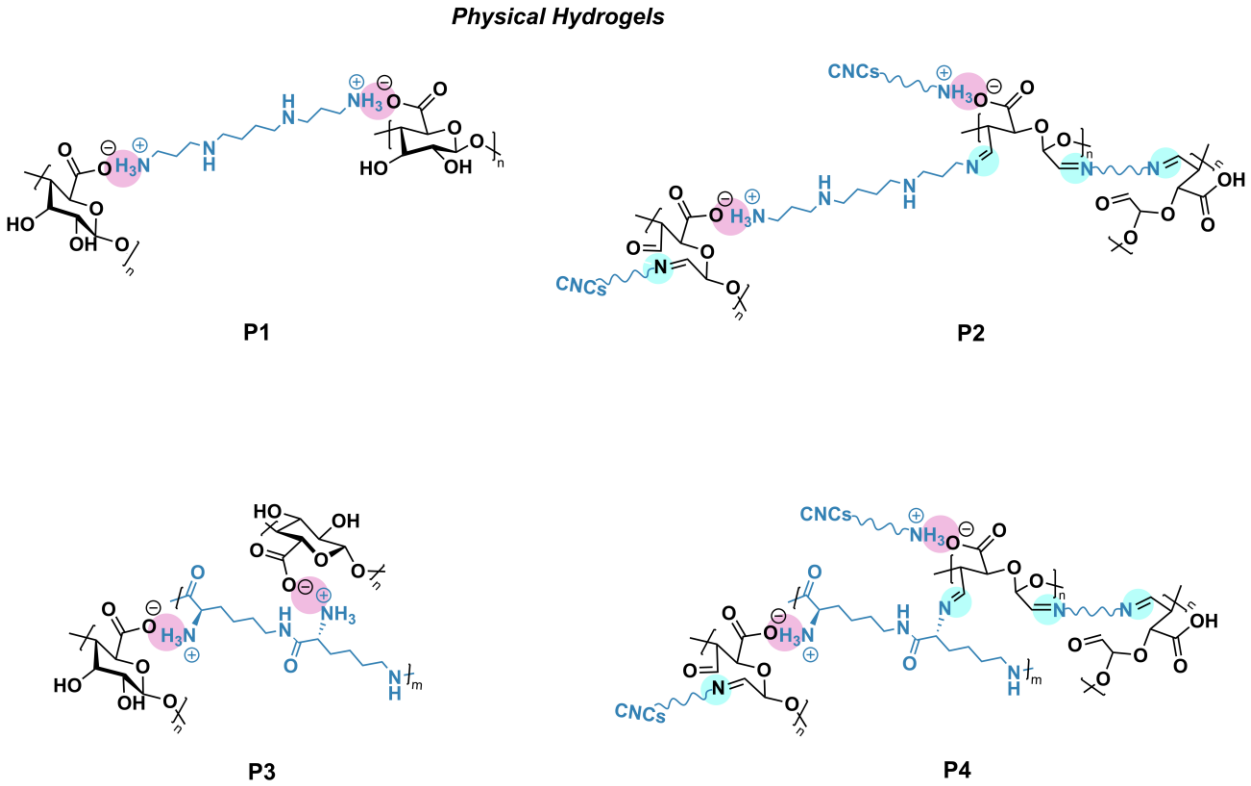

Fig. S6 *Structures of all physical hydrogels. P1 and P2 presented spermine as crosslinker, whereas P3 and P4 ε-poly-L-lysine; in P1 and P3 nanocellulose is mono-oxidized (CNCs-COOH), while P2 and P4 nanocellulose is bi-oxidized (CNCs-COOH-CHO).*

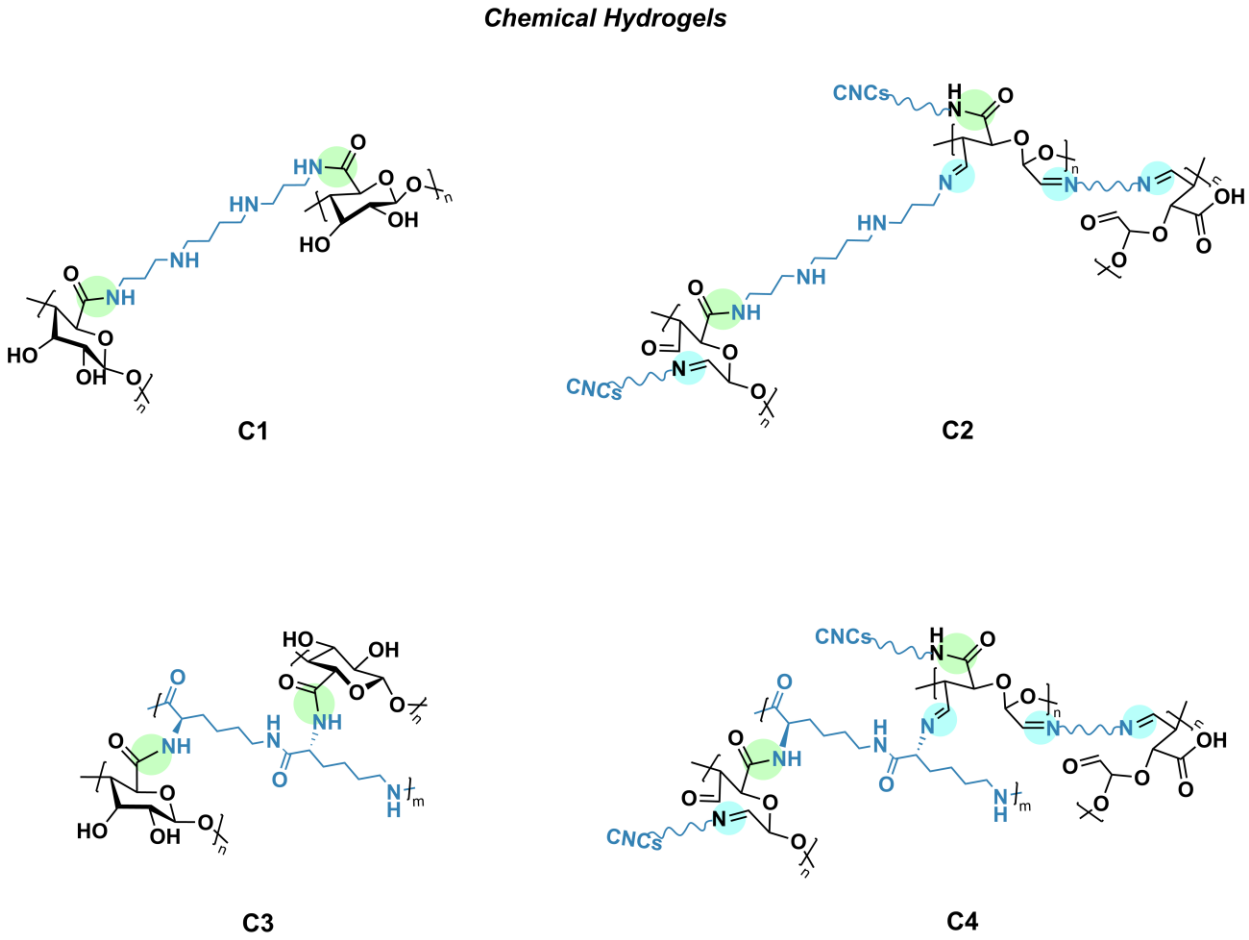

Fig. S7 *Structures of all chemical hydrogels. C1 and C2 presented spermine as crosslinker, whereas C3 and C4 ε-poly-L-lysine; in C1 and C3 nanocellulose is mono-oxidized (CNCs-COOH), while C2 and C4 nanocellulose is bi-oxidized (CNCs-COOH-CHO).*

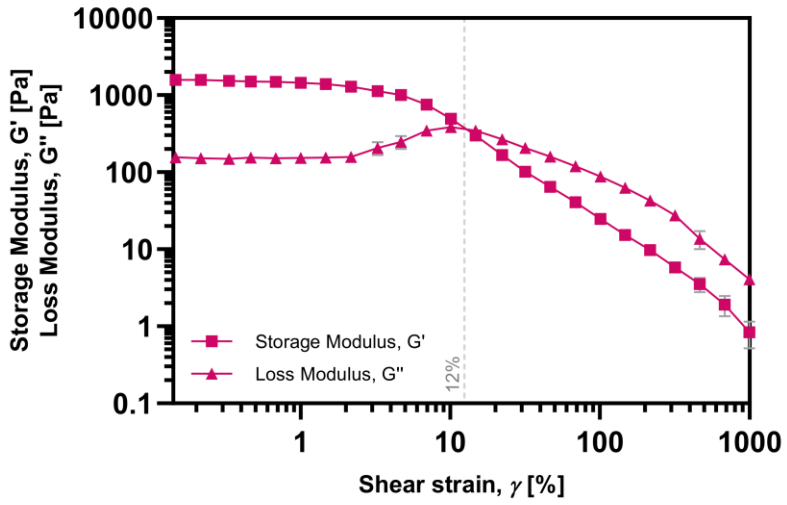

Fig. S8 *Amplitude sweep test curve for a gel formulated using CNCs-COOH with a carboxylic acids content equal to 0.09 ± 0.02 mmol/g. Breaking point of the gel is at 12% shear strain.*

Reference ATR-FTIR spectra and additional band assignments. Reference ATR-FTIR spectra of the pristine crosslinkers were collected to identify their diagnostic vibrational features and to facilitate the interpretation of the spectral changes which occur upon hydrogel assembly. Figure S9 reports the spectra of spermine and ε-poly-L-lysine. Spermine shows typical vibrational features in the 1050–1150 cm^{-1} region (C–N stretching) and in the 2800–2950 cm^{-1} region (C–H stretching).[4] The ε-poly-L-lysine spectrum reflects the presence of isopeptide bonds between the α-carboxyl group and the ε-amino group, with amide III (C–N stretching + N–H bending), amide II (N–H bending + C–N stretching) and amide I (C=O stretching) bands at 1250, 1531 and 1649 cm^{-1}, respectively;[5,6] additionally, a broad absorption band in the 3200–3300 cm^{-1} range is observed, corresponding to N–H stretching vibrations.

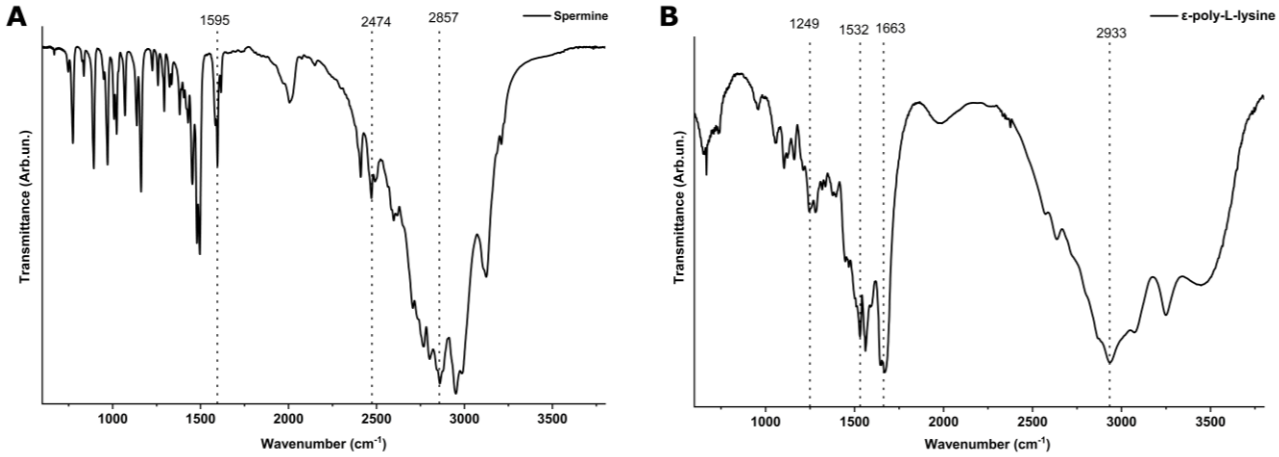

Fig. S9 *The ATR-FTIR spectra of the starting materials:* ***(A)*** *Spermine,* ***(B)*** *ε-poly-L-lysine.*

Table S6 *Main diagnostic ATR-FTIR bands of the pristine crosslinkers.*

Compound	Wavenumber (cm^{-1})	Assignment
Spermine	1050–1150	C–N stretching
Spermine	2800–2950	C–H stretching
ε-poly-L-lysine	1250	Amide III (C–N stretching + N–H bending)
ε-poly-L-lysine	1531	Amide II (N–H bending + C–N stretching)
ε-poly-L-lysine	1649	Amide I (C=O stretching)
ε-poly-L-lysine	3200–3300	N–H stretching (broad band)

In physically crosslinked hydrogels, minor contributions from the crosslinkers remain visible. For example, in P1 bands attributable to spermine are observed at 2408, 2471 and 2858 cm-1 (as indicated in Fig. 4A). Carbonyl-related bands characteristic of spermine (~1595 cm-1) and ε-poly-L-lysine (~1664 cm-1) are also detectable in the spectra of P1 and P3. A complete list of peak positions and assignments for the pristine crosslinkers and for all hydrogel

formulations is provided in Table S7.

Table S7 *Assignment of the main ATR-FTIR absorption bands observed for pristine components and hydrogel formulations in P and C series.*

Wavenumber (cm^{-1})	Assignment	Vibrational mode	Observed in
3330–3350	O–H / N–H stretching	Hydrogen-bonded hydroxyl and amine stretching	CNCs, P1–P4, C1–C4
3200–3300	N–H stretching	Amine / amide N–H stretching	ε-poly-L-lysine, hydrogels
2950–2800	C–H stretching	Aliphatic C–H stretching	Spermine, hydrogels
2858	C–H stretching	$–CH_2$ symmetric stretching	Spermine, P1
2470–2400	$N–H^+$ vibrations	Protonated amine groups	Spermine, P1
1720–1700	C=O stretching	Aldehyde / carboxylic acid carbonyl	CNCs-COOH-CHO
1665–1645	Amide I	C=O stretching (amide)	ε-poly-L-lysine, C1–C4
1650–1640	C=O stretching (shifted)	$COO^–$–NH_3^+ electrostatic interactions	P1, P3
1595	C=O / $COO^–$ asym. stretching	Carboxylate groups	Spermine-containing systems
1555–1530	Amide II	N–H bending + C–N stretching	ε-poly-L-lysine, C1–C4
1250	Amide III	C–N stretching + N–H bending	ε-poly-L-lysine
1150–1050	C–N stretching	Aliphatic amine vibrations	Spermine
~1050	C–O stretching	Polysaccharide backbone	CNC-based samples

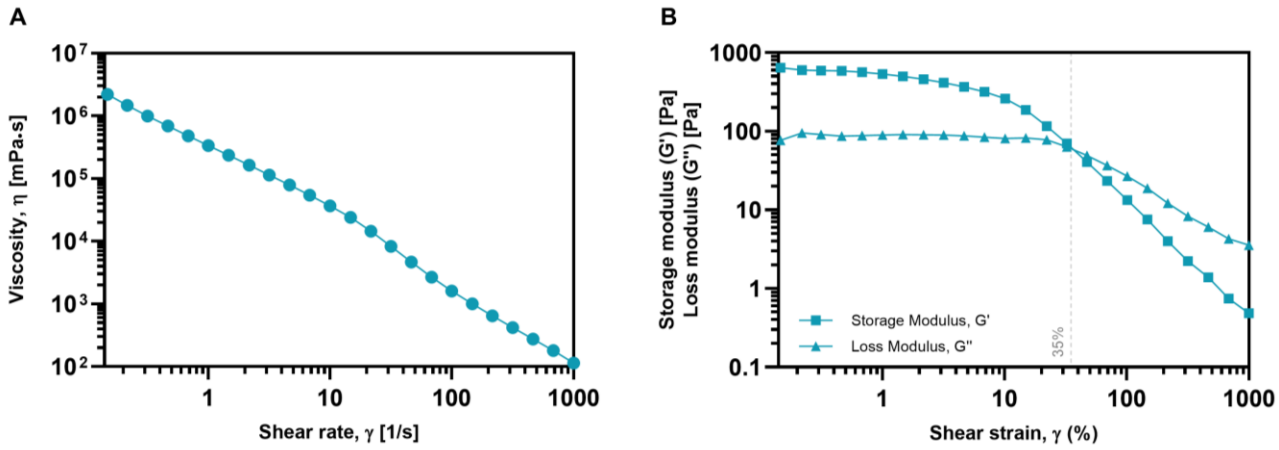

Fig. S10 (A) *Viscosity measurements of C3 hydrogel.* ***(B)*** *Amplitude sweep tests repeated on C3 hydrogel after the experiment performed to measure viscosity (injectability test).*

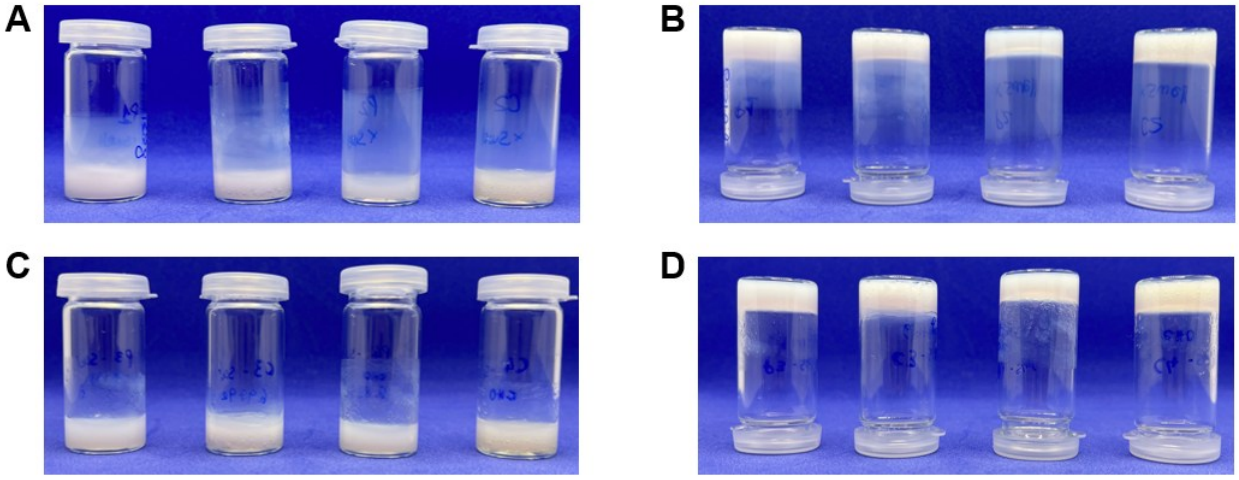

Fig. S11 *Tilt test evaluation. (A) Spermine hydrogels: from left to right P1, C1, P2, and C2. (B) Tilt-test of spermine hydrogels. (C) ε-poly-L-lysine hydrogels: from left to right P3, C3, P4, and C4. (D) Tilt-test of ε-poly-L-lysine hydrogels.*

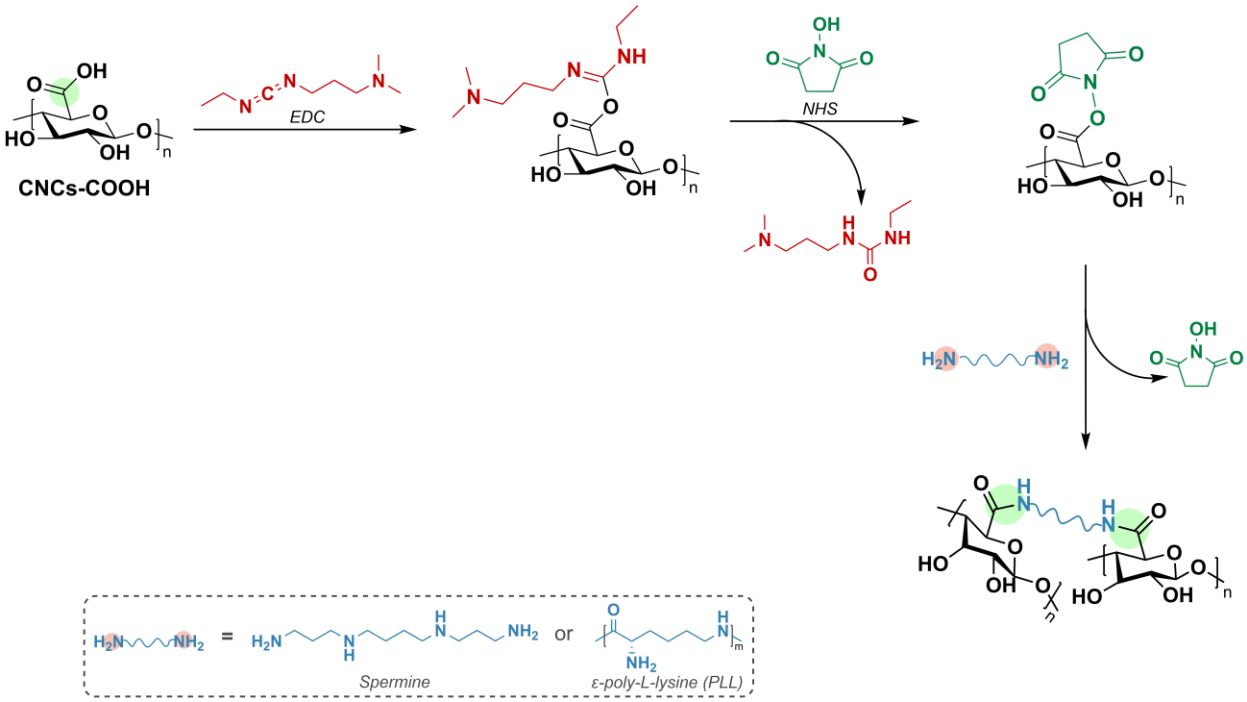

Fig. S12 *EDC/NHS coupling reaction to conjugate carboxylic acids to amines in aqueous conditions.*

Table S8 *Representative concentrations from the tested range for physically crosslinked hydrogels. Lower concentrations of the starting CNCs-COOH or CNCs-COOH-CHO and their corresponding combinations with crosslinkers are not included in this table, as gelation was not achieved or only highly fluid systems were obtained under those conditions. Gelation results of the optimised hydrogels are highlighted in green.*

	Physical hydrogels		
	Spermine (% w/w)	**ε-Poly-L-lysine (% w/w)**	**Gelation results**
CNCs-COOH 4.5% w/w	0.4	–	Absence of gelation
	1	–	Too liquid
	2	–	Soft gel
	2.5	–	Creamy gel
CNCs-COOH 5% w/w	–	0.08	Too creamy, weak gel
	–	0.1	Weak gel
	–	0.2	Creamy, smooth gel
	–	0.8	Gel shrinkage
CNCs-COOH-CHO 4.5% w/w	0.4	–	Gel not formed
	1	–	Weak gel, poorly defined edges
	2	–	Rigid gel, partially defined edges
	2.5	–	Jelly-like, shape-retaining gel
CNCs-COOH-CHO 5% w/w	–	0.08	Weak gel
	–	0.1	Solid gel, relatively defined edges
	–	0.2	Well-defined edges, self-supporting gel

Table S9 *Selected concentrations from the wide range of concentrations screened to formulate chemical hydrogels. Lower concentrations of the precursor CNCs-COOH or CNCs-COOH-CHO and their related formulations with crosslinkers are not presented in this table, as gel formation did not occur or only very fluid systems were obtained under those conditions. The gelation outcomes of the optimized formulations are highlighted in green.*

	Chemical hydrogels		
	Spermine (% w/w)	**ε-Poly-L-lysine (% w/w)**	**Gelation results**
CNCs-COOH 3.5% w/w	0.1	–	Gel not formed
	0.2	–	Too liquid
	0.4	–	Too creamy
	1	–	Unsuccessful gelation
CNCs-COOH 4% w/w	0.1	–	Too creamy, weak gel
	0.2	–	Rigid, shape-retaining gel
	0.4	–	Gel shrinkage
CNCs-COOH 5% w/w	–	0.08	Too creamy
	–	0.1	Creamy, soft gel
	–	0.2	Gel shrinkage
	–	0.4	Gel syneresis
CNCs-COOH-CHO 4% w/w	0.1	–	Jelly-like, moderately defined edges
	0.2	–	Well-defined edges, self-supporting gel
	0.4	–	Too rigid
CNCs-COOH-CHO 3.5% w/w	–	0.05	Absence of gelation
	–	0.1	Weak gel
	–	0.2	Stiff, self-standing gel
	–	0.4	Too brittle

A

Standard	[Doxo] µM/mL	Peak Area (mAu·s)
Std 1	0.10	0.400
Std 2	0.20	0.791
Std 3	0.40	1.696
Std 4	0.80	3.727
Std 5	1.50	6.632
Std 6	3.00	13.195

B

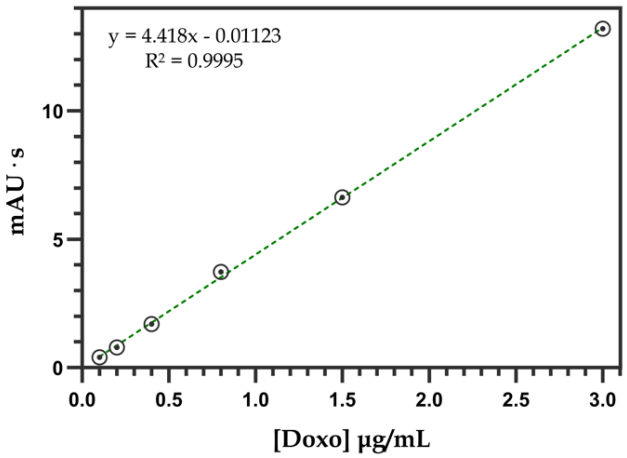

Fig. S13 (A) *Doxorubicin standard solutions' concentration and the corresponding HPLC peak area.* ***(B)*** *Calibration line used for doxorubicin release quantification through HPLC-MS with the corresponding curve equation and R^2.*

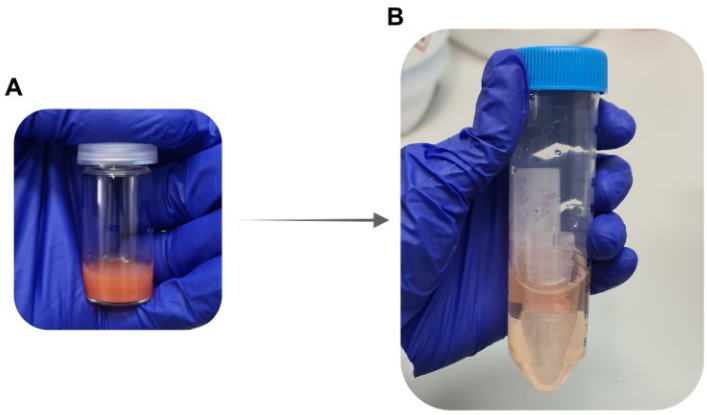

Fig. S14 (A) *Drug loading of C4 hydrogel.* ***(B)*** *Drug release in PBS carried out by transferring the loaded hydrogel inside a D-Tube Dialyzer Midi (MWCO 3.5 kDa) device and immersing it in buffer.*

References

1 R. S. Dassanayake, N. Dissanayake, J. S. Fierro, N. Abidi, E. L. Quitevis, K. Boggavarappu and V. D. Thalangamaarachchige, Characterization of cellulose nanocrystals by current spectroscopic techniques, *Appl. Spectrosc. Rev.*, 2023, **58**, 180–205.

2 F. Cheng, P. Zhao, T. Ouyang, J. Sun and Y. Wu, Comprehensive utilization strategy of cellulose in a facile, controllable, high-yield preparation process of cellulose nanocrystals using aqueous tetrabutylphosphonium hydroxide, *Green Chemistry*, 2021, **23**, 1805–1815.

3 E. S. Madivoli, P. G. Kareru, A. N. Gachanja, S. M. Mugo and D. S. Makhanu, Synthesis and characterization of dialdehyde cellulose nanofibers from O. sativa husks, *SN Appl. Sci.*, 2019, **1**, 723.

4 A. Bertoluzza, C. Fagnano, P. Finelli, M. A. Morelli, R. Simoni and R. Tosi, Raman and infrared spectra of spermidine and spermine and their hydrochlorides and phosphates as a basis for the study of the interactions between polyamines and nucleic acids, *Journal of Raman Spectroscopy*, 1983, **14**, 386–394.

5 J.-N. Liu, S.-L. Chang, P.-W. Xu, M.-H. Tan, B. Zhao, X.-D. Wang and Q.-S. Zhao, Structural Changes and Antibacterial Activity of Epsilon-poly- <scp>l</scp> -lysine in Response to pH and Phase Transition and Their Mechanisms, *J. Agric. Food Chem.*, 2020, **68**, 1101–1109.

6 M. Nochi, Y. Ozaki and H. Sato, Water-induced conformational changes in the powder and film of ε-poly(L)lysine studied by infrared and Raman spectroscopy, *Spectrochim. Acta A Mol. Biomol. Spectrosc.*, 2021, **260**, 119900.